Structural and magnetic characterization of Co_xNi_{1-x} nanoparticles in yttria-stabilized zirconia single crystals

S. Zhu and K. Sun
Department of Nuclear Engineering and Radiological Sciences, University of Michigan, Ann Arbor, Michigan 48109

Q. Y. Zhang
State Key Laboratory for Materials Modification by Laser, Ion and Electron Beams, Department of Physics, Dalian University of Technology, Dalian 116024, People's Republic of China

X. T. Zu
Department of Applied Physics, University of Electronic Science and Technology of China, Chengdu 610054, People's Republic of China

L. M. Wang[a] and R. C. Ewing
Department of Nuclear Engineering and Radiological Sciences, University of Michigan, Ann Arbor, Michigan 48109

(Received 22 May 2003; accepted 10 August 2003)

Oriented Co_xNi_{1-x} nanoparticles were synthesized by sequential implantation of 90 keV Co and Ni ions at room temperature in the near surface of an yttria-stabilized zirconia single crystal. Transmission electron microscopy and a superconducting quantum interference device magnetometer as well as a vibrating sample magnetometer were utilized to characterize the structural and magnetic properties of the implanted layer. Typical nanoparticles range from 3 to 10 nm in diameter, and some elongated precipitates as long as 25 nm were formed by joining the nanoparticles with nanotwins. Hysteresis loops were measured at both 300 and 10 K, and showed coercivity of 100 or 250 Oe, respectively. Magnetization versus temperature in zero-field-cooled and field-cooled fields was measured. No obvious superparamagnetism was detected below 300 K. [DOI: 10.1063/1.1615299]

I. INTRODUCTION

Nanometer-sized metallic crystallites embedded in a dielectric matrix have attracted considerable attention during the past decade because of their numerous technological applications.[1] These materials when implanted with metallic ions exhibit very interesting optical, electronic, and ferromagnetic properties that are different from those of the bulk matrix. Nanocomposites of Au, Ag, and Cu in TiO_2 or MgO with surface plasmon effects and nonlinear optical properties have been reported.[2,3] Nanocomposites of ferromagnetic CoCu in a nonmagnetic host exhibit giant magnetoresistance (GMR) and may have application in magnetic recording heads.[4] Ferromagnetic metallic nanoparticles (Fe/Pt, Co/Pt, Ni) in insulating matrices SiO_2, Al_2O_3, yttria-stabilized zirconia (YSZ), and ZnO exhibit interesting magnetic properties, and they may be candidates for magnetic information storage media.[5–9] Among the various experimental techniques employed to synthesize nanoparticles in the near surface, ion implantation is one of most promising methods because implanted ions frequently precipitate as nanoparticles in controlled concentrations at precalculated depths of the host matrix. In this study, a nanocomposite of Co_xNi_{1-x} particles embedded in optically active YSZ was fabricated by ion implantation for potential application in magneto-optical devices. The structural and magnetic properties were characterized by transmission electron microscopy (TEM) and magnetometers.

II. EXPERIMENTAL METHODS

A well-polished (001) oriented YSZ (with 9.5 mol % Y_2O_3) single crystal was sequentially implanted with 90 keV Co ions followed by 90 keV Ni ions to a fluence of $1\times10^{17}/cm^2$ each. Ion implantation was conducted at room temperature using a metal vacuum vapor arc (MEVVA) 80-10 implanter. The flux was 2.9×10^{13} ions/cm^2 s for Co ions and 2.6×10^{13} ions/cm^2 s for Ni ions, respectively. The maximum temperature during implantation was monitored to be less than 140 °C. SRIM2000 was used to calculate the level of damage.[10] The morphology and structure of the nanoparticles were characterized by TEM using a JEOL 2010 field emission gun (FEG) at 200 keV. The magnetic properties of the samples were characterized by a multiphonon mass spectrometer (MPMS) superconducting quantum interference device (SQUID) magnetometer at 10 K and a vibrating sample magnetometer at 300 K. The zero-field-cooling (ZFC) and field-cooling (FC) curves were measured by cooling the sample initially in zero field to 10 K, and the magnetization was recorded in a magnetic field where $H=100$ Oe as the temperature was increased. When the temperature reached

[a]Author to whom correspondence should be addressed; electronic mail: lmwang@umich.edu

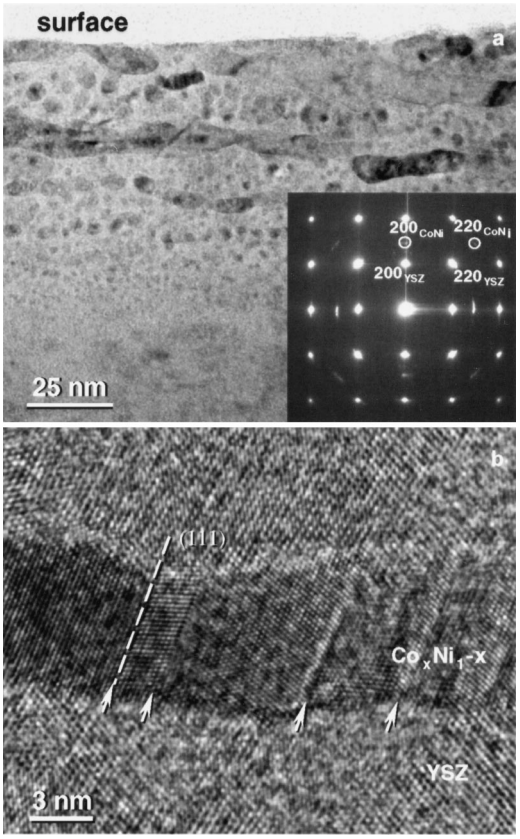

FIG. 1. Bright-field cross-sectional TEM (a) and high resolution TEM (b) micrographs showing nanoparticles of Co_xNi_{1-x} in the near surface of a YSZ single crystal; SAD pattern [inset in (a)] indicating the orientation of the nanoparticles to the matrix.

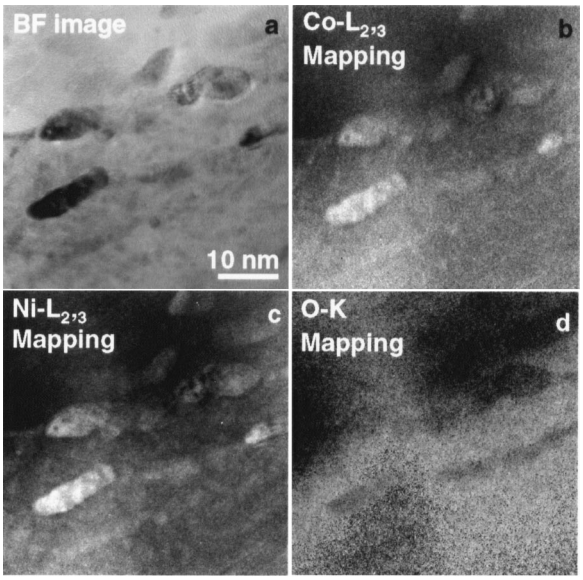

FIG. 2. (a) Bright-field image and elemental mapping images of (b) Co, (c) Ni, and (d) O, respectively, indicating the compositional distribution of the nanoparticles.

300 K, the sample was gradually cooled, and the magnetization was recorded. The magnetization as a function of magnetic field was measured at both 300 K and 10 K.

III. RESULTS AND DISCUSSION

A bright field cross-sectional TEM image [Fig. 1(a)] shows that the nanoparticles precipitated spontaneously during ion implantation from the surface of the YSZ matrix to a depth of 80 nm, which is the projected range of the implanted Co and Ni with 90 keV in YSZ according to the results calculated by SRIM2000. This confirmed that surface sputtering of the matrix was not significant.[11] The typical nanoparticle size ranged from 3 to 10 nm. In the high concentration region of implanted Co and Ni ions (~25–40 nm below the surface), some large precipitates up to 25 nm in length formed parallel to the surface of YSZ. High-resolution TEM images clearly revealed that the elongated particles consisted of individual crystals joined across twin boundaries. The (111) twin planes are shown in Fig. 1(b). The selected area diffraction (SAD) pattern in Fig. 1(a) exhibits obvious extra diffraction spots from the precipitates, which are circled in the SAD pattern. The precipitates are cubic with $a \cong 0.35$ nm. The phases consistent with this lattice parameter include cubic Co, Ni, solid solution Co_xNi_{1-x}, as well as intermetallic phases, CoNi and Co_3Ni_7.[12] Energy-filtered elemental mapping images of Co, Ni, and O using the $L_{2,3}$ or K edges in a corresponding energy electron-loss spectroscopy (EELS) spectrum, are shown in Fig. 2. The bright contrast of the nanoparticles in the Co and Ni maps indicates that the nanoparticles contained both Co and Ni. These nanoparticles do not contain oxygen as indicated by the dark contrast in nanoparticles in the O map image. Energy dispersive spectroscopy (EDS) analysis showed the composition ratio of Co over Ni ranges from 0.8 to 1. Therefore, the nanoparticles are Co_xNi_{1-x} solid solution. The orientation relationship between aligned nanoparticles and the YSZ matrix are $(200)_{YSZ} \| (200)_{Co_xNi_{1-x}}$, and $[011]_{YSZ} \| [011]_{Co_xNi_{1-x}}$. Based on calculations using the SRIM code, the maximum level of damage reached 300 dpa in the YSZ matrix; however, the YSZ matrix still retained its crystallinity.

Magnetization plots as a function of magnetic field at both 10 and 300 K are shown in Fig. 3. The magnetization field H applied is parallel to (001) of the YSZ single crystal, i.e. (001) of Co_xNi_{1-x}, due to its orientation alignment. The coercivity, H_c, at 300 K was measured to be ~100 Oe. The coercivity increased to 260 Oe as the temperature decreased to 10 K. These values are consistent with previously reported particle-size dependent coercive forces in CoNi alloys.[13,14] The magnetization curves at 10 and at 300 K were completely saturated at applied fields of $H = 800$ and 5000 Oe, respectively. The saturation magnetization, M_s, increased 15% as the temperature decreased from 300 to 10 K. The remanent magnetization M_r/M_s was 0.41 at 300 K and its value increased to 0.77 at 10 K.

The variation of coercivity strongly depends on the grain size. Since nanoparticles less than a critical size are in single domain states, their coercivities are higher than that of a common bulk sample.[15] Previous investigations reported that the critical size with the largest coercivity lies in the 30–40 nm range for $Co_{50}Ni_{50}$.[13] The coercivity of our samples can

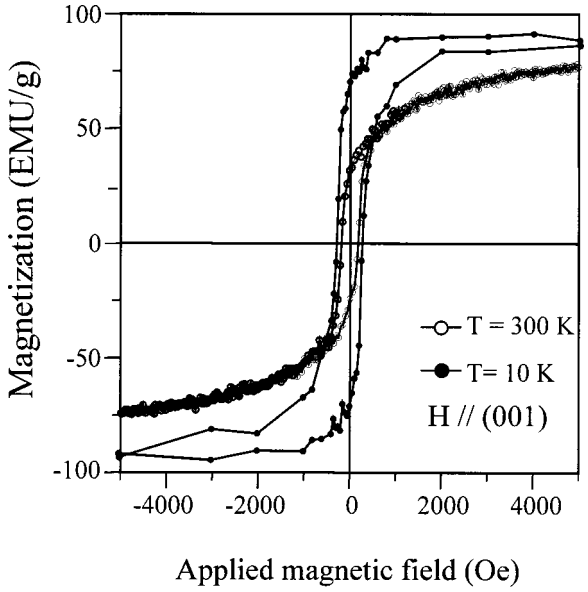

FIG. 3. Magnetization vs field applied at temperatures of 10 and 300 K. The field applied is parallel to the (001) plane of the YSZ matrix.

be attributed to this nanostructural effect. The mismatch between the matrix and the implanted Co_xNi_{1-x} particles probably induces stress, which also affects the coercivity.[16]

Nanoparticles are expected to illustrate superparamagnetic properties.[17] The critical temperature, i.e., the blocking temperature, is roughly given as[17]

$$T_b = \frac{K_{\text{eff}} V}{25 k_B}, \tag{1}$$

where K_{eff} is the effective anisotropy constant, which is related to the magnetrocrystalline anisotropy, shape anisotropy, and surface effect of the particles. V is the volume of the particle; k_B is the Boltzmann constant. The blocking temperature can be readily characterized by ZFC and FC magnetization. Figure 4 shows the temperature dependent magnetization curves under ZFC and FC processes at $H = 100$ Oe. No blocking temperature within 300 K was observed. Since TEM analysis has confirmed that the nanoparticles are not oxidized, the results from the ZFC and FC curves suggest that the sample might not be blocked at low temperature. This is reasonable if particle-size and shape effects are considered. As observed in the TEM micrograph (Fig. 1), the particle size is widely distributed from 3 to 10 nm, and some longer particles up to 25 nm have formed from a sequence of twin planes roughly perpendicular to the length of the particle. They might not be in single domain states. The blocking temperatures therefore are different and may overlap. Based on Eq. (1), $T_b \approx 227$ K, if we use the magnetocrystalline constant K_1 value (1.5×10^5 J/m^3) from Ref. 18 for K_{eff} and a maximum diameter of 10 nm for the nanoparticles. The result of this calculation differs from the experimental observation because K_1 only represents the magnetocrystalline anisotropy contribution. Since some nanoparticles are not truly spherical, the contribution by shape anisotropy to K_{eff} should also be considered. On the other hand, the elongated particles formed by repeating twins may result in interparticle dipolar interactions. Thus, supermagnetism of the Co_xNi_{1-x} nanoparticles may persist to above 300 K, and the nanoparticles will remain ferromagnetic at room temperature.

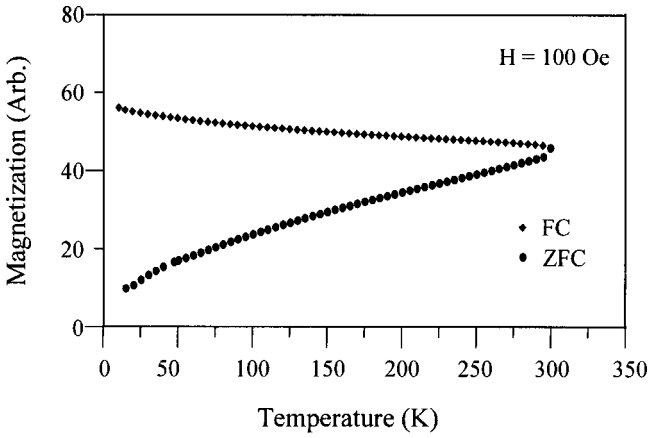

FIG. 4. Temperature dependence of the magnetization. The curves show that in the ZFC and FC processes at $H = 100$ Oe.

In conclusion, Co_xNi_{1-x} magnetic nanoparticles were synthesized using ion implantation of the near surface of YSZ single crystals. The structural and magnetic properties were characterized by TEM and magnetic measurements, respectively. Further studies with different implantation doses followed by annealing processes are being undertaken to control the particle size and to modify the magnetic properties.

ACKNOWLEDGMENTS

The TEM analysis was conducted in the Electron Microbeam Analysis Laboratory at the University of Michigan, and the authors acknowledge support of NSF Award No. DMR-9371177. This work is supported by US Department of Energy under Grant Nos. DE-FG02-97ER45656 and DF-FG02-02ER46005.

[1] A. Meldrum, R. F. Haglund, Jr., L. A. Boatner, and C. W. White, Adv. Mater. (Weinheim, Ger.) **13**, 1431 (2001).
[2] P. Galletto, P. F. Brevet, H. H. Girault, R. Antoine, and M. Broyer, J. Phys. Chem. B **103**, 8706 (1999).
[3] G. De Marchi, F. Gonella, P. Mazzoldi, G. Battaglin, E. J. Knystautas, and C. Meneghini, J. Non-Cryst. Solids **196**, 79 (1996).
[4] J. Q. Xiao, J. S. Jiang, and C. L. Chien, Phys. Rev. Lett. **68**, 3749 (1992).
[5] C. E. Vallet, C. W. White, S. P. Withrow, J. D. Budai, L. A. Boatner, K. D. Sorge, J. R. Thompson, K. S. Beaty, and A. Meldrum, J. Appl. Phys. **92**, 6200 (2002).
[6] B. Bian, Y. Hirotsu, K. Sato K, T. Ohkubo, and A. Makino, J. Electron Microsc. **48**, 753 (1999).
[7] S. Honda, F. A. Modine, A. Meldrum, J. D. Budai, T. E. Haynes, and L. A. Boatner, Appl. Phys. Lett. **77**, 711 (2000).
[8] S. P. Withrow, C. W. White, J. D. Budai, L. A. Boatner, K. D. Sorge, J. R. Thompson, and R. Kalyanaraman, J. Magn. Magn. Mater. **260**, 319 (2003).
[9] L. Takacs, M. Pardavi-Horvath, J. Appl. Phys. **75**, 5864 (1994).
[10] J. F. Ziegler, *The Stopping and Range of Ions in Matter* (IBM Research, Yorktown, NY, 2000).
[11] I. V. Afanasyev-Charkin and K. E. Sickafus, J. Nucl. Mater. **306**, 112 (2002).
[12] P. Villars and L. D. Calvert, *Peason's Handbook of Crystallographic Data for Intermetallic Phases* (ASM, Materials Park, OH, 1991), Vol. 2.
[13] P. Toneguzzo, O. Acher, G. Viau, A. Pierrard, F. Fievet-Vincent, F. Fievet, and I. Rosenman, IEEE Trans. Magn. **35**, 3469 (1999).

[14] C. de Julián *et al.*, J. Magn. Magn. Mater. **226–230**, 1912 (2001).
[15] D. L. Leslie-Pelecky, Chem. Mater. **8**, 1770 (1996).
[16] M. P. Morales, M. J. Munoz-Aguado, J. L. Garcia-Palacios, F. J. Lazaro, and C. J. Serna, J. Magn. Magn. Mater. **183**, 232 (1998).
[17] F. C. Fonseca, G. F. Goya, R. F. Jardim, R. Muccillo, N. L. V. Carreno, E. Longo, and E. R. Leite, Phys. Rev. B **66**, 104406 (2002).
[18] *Magnetic Properties of Metals*, edited by H. P. J. Wijn (Springer, Berlin, 1991), p. 22.